SYNTHESIS OF NONLINEAR SYSTEMS HAVING

PRESCRIBED PERIODIC SOLUTIONS

by

L. O. Chua and D. N. Green

Memorandum No. ERL-M350

16 August 1972

ELECTRONICS RESEARCH LABORATORY

College of Engineering
University of California, Berkeley
94720

SYNTHESIS OF NONLINEAR SYSTEMS HAVING PRESCRIBED PERIODIC SOLUTIONS

L. O. Chua and D. N. Green†

ABSTRACT

Methods for synthesizing an autonomous nonlinear system having prescribed periodic solutions are presented. The methods are based on the observation that any periodic function

$$x(t) = a_0 + \sum_{k=1}^{m} [a_k \cos k\omega t + b_k \sin k\omega t]$$

can be expressed as a polynomial of cos ωt and sin ωt, where ω is the fundamental frequency. A second-order differential equation is developed whose globally-stable limit cycle solution is cos ωt and sin ωt. This differential equation is combined with the polynomial to form a) a third-order differential equation which has the prescribed periodic solution as its unique steady-state solution, and b) a second-order differential equation which has the prescribed periodic solution as its unique C^1 steady-state solution.

Research sponsored in part by the U.S. Naval Electronic Systems Command, Contract N00039-71-C-0255 and the National Science Foundation, Grant GK-32236.

†The authors are with the Department of Electrical Engineering and Computer Sciences, and the Electronics Research Laboratory, University of California, Berkeley, California, 94720.

I. INTRODUCTION

Although the area of nonlinear ordinary differential equations is a highly developed discipline, it has been addressed almost exclusively to analysis problems [1-5]; namely, given a differential equation, find the solution through an initial state, or investigate the qualitative behavior of the solutions. The converse synthesis problem of finding a class of differential equations having some prescribed properties is a relatively new area in which only isolated results have been obtained [6-10]. Perhaps the earliest work addressed to the synthesis problem is due to Vallese [6] in which he proposed a class of second order systems capable of realizing a prescribed set of singular points in a limited region of the phase plane. He also proposed an approach for synthesizing a system with a limited class of prescribed periodic solutions.

The synthesis of an nth order nonlinear differential equation having a set of prescribed singular points with prescribed eigen-values has been solved recently [8]. This paper is addressed to the problem of synthesizing a system having a prescribed periodic stable solution of a prescribed frequency ω. The periodic solution is expressed as a Fourier series:

$$x(t) = \sum_{k=-\infty}^{\infty} \alpha_k e^{k(j\omega t)} \tag{1}$$

Consequently, the function must obey the Dirichlet condition: $x: \mathbb{R} \to \mathbb{R}$ is real, periodic, bounded, piecewise-continuous and has a finite number of minima, maxima and discontinuities in one period. Using the well-known mathematical fact that (1) may be uniformly approximated by a finite sum

[1], (1) reduces to

$$x(t) = a_0 + \sum_{k=1}^{m} [a_k \cos k\omega t + b_k \sin k\omega t]. \tag{2}$$

The synthesis methods of this paper are directed towards producing (2), where parameters a_k, b_k, m and ω are arbitrarily prescribed.

The synthesis problem has both theoretical and practical significance. From the theoretical standpoint, it is of particular interest to know the minimum number of state variables required by an autonomous system capable of generating an arbitrary periodic waveform. It has been shown that no first order autonomous system can oscillate [11]. It is also well known that a second order system--such as the Van der Pol equation--can generate a wide variety of periodic waveforms ranging from a pure sinusoid to an almost-square wave. However, it is not known whether a second order system, or an nth order system, can always be found which is capable of generating an arbitary periodic waveform. From the practical standpoint, the solution to this synthesis problem is fundamental to the modeling and simulation of oscillatory systems. A case in point would be the modeling of many biological systems--such as the astable membrane action potential waveforms generated by cardiac pacemaker cells [12-13]--in which the physical operating mechanism is virtually unknown and hence a black box or mathematical model seems to be the only recourse [14-15].

In Section II we present the basic method used to generate (2). Any sinusoidal waveform $\cos k\omega t$ or $\sin k\omega t$ ($k \geq 1$) can be expressed as polynomials of $\cos\omega t$ and $\sin\omega t$; in particular by the Chebyshev polynomials. Thus an ordinary function generator [16-17] can be used to produce $\cos\omega t$ and $\sin\omega t$

which are then multiplied by analog multipliers. This process is discussed in detail.

In Section III we present two autonomous systems used to generate $\cos\omega t$ and $\sin\omega t$. System $\hat{S}(p,x_2)$ is a second-order, real, autonomous differential equation whose non-constant solutions assymptotically approach the desired waveforms. System $\hat{S}(p,x_2,x_3)$ is a third-order differential equation with essentially the same properties as $\hat{S}(p,x_2)$.

In Section IV we demonstrate that the Chebyshev polynomials can be used to form a C^∞ diffeomorphic onto function γ: $\mathbb{R}^3 \to \mathbb{R}^3$. This function converts $\hat{S}(p,x_2,x_3)$ into another System $S(x_1,x_2,x_3)$ which is a third-order differential equation whose non-constant solutions asymptotically approach (2).

In Section V we use the Chebyshev polynomials to form a C^∞ function η: $\mathbb{R}^2 \to \mathbb{R}^2$. In general, η is not bijective and it is not possible to transform $\hat{S}(p,x_2)$ into a well-defined differential equation. Instead we define system $S(x_1,x_2)$ to be trajectories in $\mathbb{R}^2$ which are the η-images of trajectories generated by $\hat{S}(p,x_2)$. The non-diffeomorphic nature of η manifests itself in the trajectories of $S(x_1,x_2)$: There exist lines in $\mathbb{R}^2$ called <u>barrier lines</u> and each barrier line intersects all trajectories at exactly one point, called the <u>tunnel point</u>.

Under rather rigid conditions, the function η is bijective (hence C^∞ diffeomorphic and onto). Thus there exists a second-order differential equation whose solutions are the trajectories of $S(x_1,x_2)$. If η is not bijective, this differential equation is not defined along the barrier lines. However, it is shown that the trajectories of $S(x_1,x_2)$ are the <u>unique</u> C^1 functions satisfying the differential equation everywhere except at the tunnel points where it is not defined.

II. TRANSFORMING A SINUSOIDAL WAVEFORM INTO A PRESCRIBED PERIODIC WAVEFORM

It is possible to use the functions cos ωt and sin ωt in polynomial form to express periodic functions having frequency kω, where k is a positive integer. Define

$$T_k(x) \triangleq \frac{k}{2} \sum_{j=0}^{\left[\frac{k}{2}\right]} (-1)^j \frac{(k-j-1)!}{j!(k-2j)!} (2x)^{k-2j} \qquad (3)$$

$$U_k(x) \triangleq \sum_{j=0}^{\left[\frac{k}{2}\right]} (-1)^j \frac{(k-j)!}{j!(k-2j)!} (2x)^{k-2j} \qquad (4)$$

where $T_k(\cdot)$ and $U_k(\cdot)$ are the kth Chebyshev polynomials of the first and second kind respectively [18], and

$$\cos(k\theta) = T_k(\cos\theta) \qquad (5)$$

$$\sin(k\theta) = \sin\theta \; U_{k-1}(\cos\theta) \qquad (6)$$

Equation (2) becomes

$$x(t) = a_0 + \sum_{k=1}^{m} [a_k T_k(\cos\omega t) + b_k \sin\omega t \; U_{k-1}(\cos\omega t)] \qquad (7)$$

The most direct application of (7) is to use an ordinary function generator [16] to produce a sinusoidal waveform. This waveform is integrated and scaled to produce cosine and sine waveforms of unit amplitude.

The resulting waveforms are multiplied in the manner of (7). The block diagram illustrating this process is shown in Figure 1a. The following is a detailed description of the process.

Block 1: See Figure 2. This block consists of multipliers, an integrator, an amplitude detector and an inverse block. The inverse Block can be realized by an operational amplifier-analog multiplier, divider circuit [17]. The integrator is an operational amplifier with capacitive feedback. The amplitude detector is any device which senses the amplitude of a sinusoidal waveform.

Block 2: See Figure 3. This block is used to generate the Chebyshev polynomials and consists of multipliers[1] and operational amplifiers.

The most sensitive part of the system described above is the creation of the waveforms cos ωt and sin ωt. If the waveform cos ωt has other than unit amplitude, the amplitude error is magnified by the multiplication process in Block 2. If the waveform $A\cos(\omega t)$ entering the integrator has a net A.C. or D.C. drift component, the output of the integrator will not be a sinusoid. While there are other ways to synthesize Block 1, it is desirable to have an <u>autonomous</u> method to generate cos ωt and sin ωt; see Figure 1b. This method is described in Section III. Throughout the remainder of this paper, synthesis methods are developed entirely in the form of differential equations. To conserve space block diagrams such as Figures 2 and 3 are not explicitly given.

[1] Precision analog multipliers in integrated circuit form are now available at low cost. In fact, an array of multipliers as shown in Figure 3 could be integrated in a monolithic chip.

III. AUTONOMOUS GENEATION OF SINUSOIDAL WAVEFORMS

In this section we develop methods for generating unit amplitude waveforms cos ωt and sin ωt. In keeping with the remarks of Section II, these functions are unique in the sense that no other steady-state waveform is generated. As an example of a system with a unique steady-state waveform solution, examine the Van der Pol equation:

$$\dot{y}_1 = y_2 \tag{8}$$

$$\dot{y}_2 = - y_1 - \mu(y_1^2-1)y_2 \tag{9}$$

It is well-known that for any $\mu > 0$ in (9), all solutions of (8) and (9) assymptotically approach some unique periodic waveform (unless the initial condition is (0,0)) and that as $\mu \to 0$, the waveform approaches $y_1(t) = \sin t$, $y_2(t) = \cos t$. The uniqueness of the waveform is due to the existence of a globally-stable limit cycle in the y_1-y_2 phase plane. The following system $\hat{S}(p,x_2)$ is a second-order differential equation with a globally stable limit cycle described exactly by $p^2(t) + x_2^2(t) = 1$. Thus the unique periodic waveform is $p(t) = \sin \omega t$, $x_2(t) = \cos \omega t$. System $\hat{S}(p,x_2)$ is the basis of the synthesis method presented in Section V.

Define the real, second-order, autonomous system $\hat{S}(p,x_2)$:

$$\dot{p} = \omega[x_2 + p(1-p^2-x_2^2)] \tag{10}$$

$$\dot{x}_2 = \omega[- p + x_2 \ (1-p^2-x_2^2)] \tag{11}$$

Lemma 1.

The system $\hat{S}(p,x_2)$ has a unique non-constant periodic solution $p(t) = \sin(\omega t+\theta)$ and $x_2(t) = \cos(\omega t+\theta)$, where the phase angle θ depends only on the initial condition. All solutions approach this periodic solution as a limit, unless the initial condition is (0,0).

Proof. The point (0,0) is the only equilibrium point of $\hat{S}(p,x_2)$. Excluding this point, (10) and (11) can be transformed via polar coordinates $r \triangleq \sqrt{p^2 + x_2^2}$, $\phi = \tan^{-1} \frac{p}{x_2}$ into:

$$\dot{r} = \omega r(1-r^2) \tag{12}$$

$$\dot{\phi} = \omega \tag{13}$$

Excluding $r = 0$, (12) shows that $r = 1$ is the only positive value of r for which $\dot{r} = 0$. Furthermore, $\dot{r} < 0 \;\forall\; r > 1$ and $\dot{r} > 0 \;\forall\; r \in (0,1)$. Hence all solutions approach $r = 1$ as a limit. At $r = 1$, (10) and (11) become:

$$\dot{p} = \omega\, x_2 \tag{14}$$

$$\dot{x}_2 = -\,\omega\, p \tag{15}$$

Hence in the limit, we have $p(t) = \sin(\omega t+\theta)$, $x_2(t) = \cos(\omega t+\theta)$. ¤

Lemma 1 asserts that the steady-state waveform of any non-constant solution of $\hat{S}(p,x_2)$ is $p(t) = \sin \omega t$, $x_2(t) = \cos \omega t$. It is immaterial that the steady-state solution includes a constant phase angle θ. Since initial time t_0 is arbitrary, define $t_0' = t_0 - \frac{\theta}{\omega}$. Thus for each initial condition $(p(t_0'),x_2(t_0'))$, Lemma 1 implies the steady-state solution is

$p(t) = \sin \omega t$, $x_2(t) = \cos \omega t$. Thus without loss of generality, in the following applications of Lemma 1, it is implicitly assumed $\theta = 0$.

The following system $\hat{S}(p,x_2,x_3)$ augments $\hat{S}(p,x_2)$ and forms the basis of the synthesis method of Section IV.

Define the third-order, real, autonomous system $\hat{S}(p,x_2,x_3)$:

$$\dot{p} = \omega[x_2 + p(1-p^2-x_2^2)] \tag{16}$$

$$\dot{x}_2 = \omega[-p + x_2(1-p^2-x_2^2] \tag{17}$$

$$\dot{x}_3 = \omega[x_2^2 - p^2 + p\, x_2 - x_3] \tag{18}$$

<u>Lemma 2.</u>

The system $\hat{S}(p,x_2,x_3)$ has a unique non-constant periodic solution $p = \sin \omega t$, $x_2 = \cos \omega t$, and $x_3 = \sin \omega t \cos \omega t$. All solutions approach this periodic solution as a limit, except for initial condition (0,0,0).

<u>Proof</u>. Since (18) is uncoupled from (16) and (17), whose behavior is given by Lemma 1 and since (0,0,0) is the only equilibrium point, it suffices to prove $x_3 = \sin \omega t \cos \omega t$ as $t \to \infty$. In the limit, $\frac{d}{dt}(p\, x_2) = \omega[x_2^2 - p^2]$ and (18) reduces to

$$\frac{d}{dt}[x_3 - p\, x_2] = -\omega[x_3 - p\, x_2] \tag{19}$$

Thus in the limit, $x_3 = p\, x_2 = \sin \omega t \cos \omega t$. ¤

IV. A THIRD ORDER CANONIC SYSTEM

In this section we present a method used to combine $\hat{S}(p,x_2,x_3)$ and the Chebyshev polynomials into one third-order differential equation. We first develop a mathematical tool.

Define the differential equation

$$\dot{x} = f(x), \quad x \in \mathbb{R}^n \tag{20}$$

where $f\colon \mathbb{R}^n \to \mathbb{R}^n$ and $f \in C^\infty$. Since f is a C^1 function, for every $x(0) \in \mathbb{R}^n$ there exists a unique solution of (20) [1]. This solution is denoted by $\Phi(t,x(0))$; $\Phi\colon \mathbb{R} \times \mathbb{R}^n \to \mathbb{R}^n$, and Φ is called the <u>flow</u> of (20).

Let $\gamma\colon \mathbb{R}^n \to \mathbb{R}^n$ be a C^∞ diffeomorphic, onto function, with $y = \gamma(x)$.

<u>Lemma 3</u>.

The differential equation[2]

$$\dot{y} = g(y) \triangleq \left[\frac{\partial\gamma}{\partial x}\right] \cdot f(\gamma^{-1}(y)), \qquad y \in \mathbb{R}^n \tag{21}$$

has a unique solution $\Psi(t,y(0)) = \gamma(\Phi(t,\gamma^{-1}(y(0)))$ for all $y(0) \in \mathbb{R}^n$; $\Psi\colon \mathbb{R} \times \mathbb{R}^n \to \mathbb{R}^n$ is the flow of (21).

<u>Proof</u>. The function $g\colon \mathbb{R}^n \to \mathbb{R}^n$ is a C^∞ function since it is the composition of C^∞ functions. Hence the solutions to (21) exist and are unique. Function Ψ satisfies (21) and is therefore the unique solution. ¤

[2] The symbol $\frac{\partial\gamma}{\partial x}$ denotes the n×n Jacobian matrix of $\gamma(\cdot)$ evaluated at $x = \gamma^{-1}(y)$.

In order to construct a C^∞ diffeomorphic, onto function γ, it is necessary to define the following modified Chebyshev polynomial of the second kind:

$$V_k(x) \triangleq 2 \sum_{j=0}^{\left[\frac{k-1}{2}\right]} (-1)^j \frac{(k-j)!}{j!(k-2j)!} (2x)^{k-2j-1}, \quad k \geq 1 \tag{22}$$

The function $V_k(\cdot)$ obeys

$$U_k(x) = xV_k(x) + \left(-\frac{1}{2} + \frac{1}{2}(-1)^k\right)^{\frac{k-1}{2}} \tag{23}$$

Define the C^∞ function γ: $\mathbb{R}^3 \to \mathbb{R}^3$:

$$\tilde{x}_1 = a_0 + \sum_{k=1}^{m} a_k T_k(x_2) + \beta p + x_3 \sum_{k=2}^{m} b_k V_{k-1}(x_2) \tag{24}$$

$$\tilde{x}_2 = x_2 \tag{25}$$

$$\tilde{x}_3 = x_3 \tag{26}$$

where

$$\beta \triangleq \sum_{k=1}^{m} b_k \left(-\frac{1}{2} + \frac{1}{2}(-1)^k\right)^{\frac{k-1}{2}} \tag{27}$$

Define the real, third-order, autonomous system $S(x_1, x_2, x_3)$:

$$\dot{x}_1 = \omega \left\{ \beta[x_2 + p(1-p^2-x_2^2)] + \left[\sum_{k=2}^{m} b_k \, V_{k-1}(x_2) \right] [x_2^2 - p^2 - x_3 + p\, x_2] \right.$$

$$\left. + [-p + x_2(1-p^2-x_2^2)] \left[a_1 + \sum_{k=2}^{m} a_k \frac{d\, T_k(x_2)}{d\, x_2} + x_3\, b_k \frac{d\, V_{k-1}(x_2)}{d\, x_2} \right] \right\} \tag{28}$$

$$\dot{x}_2 = \omega[-p + x_2(1-p^2-x_2^2)] \tag{29}$$

$$\dot{x}_3 = \omega[x_2^2 - p^2 - x_3 + p\, x_2] \tag{30}$$

where

$$p(x_1,x_2,x_3) \triangleq \frac{1}{\beta} \left\{ x_1 - a_0 - a_1 x_2 - \sum_{k=2}^{m} [a_k\, T_k(x_2) + x_3\, b_k\, V_{k-1}(x_2)] \right\} \tag{31}$$

Theorem 1.

Let $\beta \neq 0$. Then the third order canonic system $S(x_1,x_2,x_3)$ *has a unique non-constant periodic solution*

$$x_1(t) = a_0 + \sum_{k=1}^{m} \left[a_k \cos(k\omega t) + b_k \sin(k\, \omega t) \right] \tag{32}$$

$$x_2(t) = \cos \omega t \tag{33}$$

$$x_3(t) = \sin \omega t \cos \omega t \tag{34}$$

Furthermore, this solution is globally stable in the sense that all non-constant solutions converge to (32), (33), and (34) in the steady state.

Proof. The function γ is C^∞ diffeomorphic and onto. Its inverse is given by (31), (25) and (26). Equation (24) is equivalent to (7). The proof follows from Lemma 3. ¤

Example 1. Synthesize a third order system with the periodic solution $x_1(t) = 2\cos t + \sin t + \sin 2t$. The resulting system is:

$$\dot{x}_1 = 2[x_2 + p(1-p^2-x_2^2)] + 2[x_2^2 - p^2 + p\,x_2 - x_3] + [-p + x_2(1-p^2-x_2^2)] \quad (35)$$

$$\dot{x}_2 = -p + x_2(1-p^2-x_2^2) \quad (36)$$

$$\dot{x}_3 = x_2^2 - x_1^2 + p\,x_2 - x_3 \quad (37)$$

where

$$p \triangleq x_1 - 2\,x_2 - 2\,x_3 \quad (38)$$

As an indication of the ease in which the third order system $S(x_1, x_2, x_3)$ can be applied, we simulated Example 1 on a digital computer with the output displayed on a graphics display terminal [19]. The analog system is shown in Figure 4a, and the resulting periodic waveform $x_1(t)$ is shown in Figure 4b.

Example 2. A sketch of the transmembrane action potential of the cardiac Purkinje fiber is shown in Figure 5. The waveform satisfies the Dirichlet condition, but it exhibits an almost instantaneous jump. Consequently, a large number of harmonics is required to simulate this waveform accurately.

The resulting system $S(x_1,x_2,x_3)$ was successfully synthesized with $m = 64$. From the black box point of view, this system could serve as a model of the cardiac Purkinje fiber cell.

If $\beta = 0$ in (27) it may still be possible to use Theorem 1. It has been noted in Section II that the synthesis methods are required only to reproduce the waveform (2). Generating

$$x_1(t) = a_0 + \sum_{k=1}^{m} [a_k \cos k(\omega t+\theta) + b_k \sin k(\omega t+\theta)] \tag{39}$$

where θ is any phase angle is therefore equivalent to generating (2). Define

$$\alpha \triangleq \sum_{k=1}^{m} a_k \left(-\frac{1}{2} + \frac{1}{2}(-1)^k\right)^{\frac{k-1}{2}} \tag{40}$$

Corollory 1.

If $\beta = 0$, $\alpha \neq 0$, then the equations defining $S(x_1,x_2,x_3)$ may be used to generate (39) for any phase angle $\theta \neq \pm \pi$.

Proof. By making the appropriate time translation implied by θ, the corresponding equation (2) can be altered such that the new β satisfies $\beta \neq 0$. In particular, if $\theta = -\pi/2$ then β is given by the expression (40) and $\alpha = 0$. ¤

V. A SECOND ORDER CANONIC FORM

In this section we discuss the mapping of solutions of $\hat{S}(p,x_2)$ into the desired waveform (2).

Define the C^∞ function η: $\mathbb{R}^2 \to \mathbb{R}^2$:

$$x_1 = a_0 + \sum_{k=1}^{m}\left[a_k\, T_k(x_2) + p\, b_k\, U_{k-1}(x_2)\right] \tag{41}$$

$$x_2 = x_2. \tag{42}$$

Define the set

$$\mathcal{H} \triangleq \left\{x_2 \in \mathbb{R} \;:\; \sum_{k=1}^{m} b_k\, U_{k-1}(x_2) = 0\right\} \tag{43}$$

This set has at most m-1 elements.

The function η is C^∞ diffeomorphic and onto if and only if $\mathcal{H}$ is empty. In this case η^{-1}: $\mathbb{R}^2 \to \mathbb{R}^2$ is given by

$$p = \frac{x_1 - a_0 - \sum_{k=1}^{m} a_k T_k(x_2)}{\sum_{k=1}^{m} b_k U_{k-1}(x_2)} \tag{44}$$

and (42). The requirement that $\mathcal{H}$ be empty is unduly restrictive, i.e., the requirement that γ be C^∞ diffeomorphic and onto in Section IV ($\beta \neq 0$) is equivalent to requiring only that $x_2 = 0$ is not a member of $\mathcal{H}$. Consequently let $\Phi(t,(p(0),x_2(0)))$ be the flow of $\hat{S}(p,x_2)$ and define the image of the transformation η of Φ by

$$S(x_1,x_2) = \{\Psi' : \mathbb{R} \to \mathbb{R}^2 | \Psi'(t) =$$

$$\eta(\Phi(t,(p(0),x_2(0))))\} \qquad (45)$$

We call the image of each trajectory of $\hat{S}(p,x_2)$ a <u>trajectory</u> of $S(x_1,x_2)$. In particular we call the image of the unique circular limit cycle of $\hat{S}(p,x_2)$ the <u>limit cycle</u> of $S(x_1,x_2)$. Although each trajectory of $S(x_1,x_2)$ will be shown later to correspond to a solution of a differential equation, no such assumption is implied here. The function Ψ' comprising $S(x_1,x_2)$ is defined solely as the η-mapping of the flow Φ of $\hat{S}(p,x_2)$.

The set $\mathcal{H}$ is represented in both the p-x_2 phase plane of $\hat{S}(p,x_2)$ and in the x_1-x_2 phase plane of $S(x_1,x_2)$ by the lines $x_2 = h \in \mathcal{H}$. The non-diffeomorphic nature of η manifests itself in the behavior of the trajectories $\Psi'(t)$ crossing the line $x_2 = h$.

Define the point set

$$Q \triangleq \left\{ (x_1,x_2) \in \mathbb{R}^2 : x_1 = a_0 + \sum_{k=1}^{m} a_k\, T_k(x_2),\ x_2 \in \mathcal{H} \right\} \qquad (46$$

For each line $x_2 = h$, there is exactly one point $(x_1,x_2) \in Q$.

<u>Lemma 4</u>.

Let $\Psi'(t) = (x_1(t),\ x_2(t))$ be a trajectory of $S(x_1,x_2)$ so that $x_2(\tau) = h \in \mathcal{H}$, for some $\tau \in \mathbb{R}$. Then $\Psi'(\tau) \in Q$.

<u>Proof</u>. If $x_2(\tau) \in \mathcal{H}$, then $\sum_{k=1}^{m} b_k U_{k-1}(x_2(\tau)) = 0$ and the lemma follows from (41) and (42). ¤

Lemma 4 asserts that the function η maps the lines $x_2 = h$ in the p-x_2 phase plane into the corresponding point $(x_1,x_2) \in Q$ in the x_1-x_2

V. A SECOND ORDER CANONIC FORM

In this section we discuss the mapping of solutions of $\hat{S}(p,x_2)$ into the desired waveform (2).

Define the C^∞ function η: $\mathbb{R}^2 \to \mathbb{R}^2$:

$$x_1 = a_0 + \sum_{k=1}^{m} \left[a_k T_k(x_2) + p\, b_k U_{k-1}(x_2) \right] \tag{41}$$

$$x_2 = x_2. \tag{42}$$

Define the set

$$\mathcal{H} \triangleq \left\{ x_2 \in \mathbb{R} : \sum_{k=1}^{m} b_k U_{k-1}(x_2) = 0 \right\} \tag{43}$$

This set has at most m-1 elements.

The function η is C^∞ diffeomorphic and onto if and only if $\mathcal{H}$ is empty. In this case η^{-1}: $\mathbb{R}^2 \to \mathbb{R}^2$ is given by

$$p = \frac{x_1 - a_0 - \sum_{k=1}^{m} a_k T_k(x_2)}{\sum_{k=1}^{m} b_k U_{k-1}(x_2)} \tag{44}$$

and (42). The requirement that $\mathcal{H}$ be empty is unduly restrictive, i.e., the requirement that γ be C^∞ diffeomorphic and onto in Section IV ($\beta \neq 0$) is equivalent to requiring only that $x_2 = 0$ is not a member of $\mathcal{H}$. Consequently let $\Phi(t,(p(0),x_2(0)))$ be the flow of $\hat{S}(p,x_2)$ and define the <u>image</u> of the transformation η of Φ by

$$S(x_1,x_2) = \{\Psi' : \mathbb{R} \to \mathbb{R}^2 | \Psi'(t) =$$

$$\eta(\Phi(t,(p(0),x_2(0)))\} \qquad (45)$$

We call the image of each trajectory of $\hat{S}(p,x_2)$ a trajectory of $S(x_1,x_2)$. In particular we call the image of the unique circular limit cycle of $\hat{S}(p,x_2)$ the limit cycle of $S(x_1,x_2)$. Although each trajectory of $S(x_1,x_2)$ will be shown later to correspond to a solution of a differential equation, no such assumption is implied here. The function Ψ' comprising $S(x_1,x_2)$ is defined solely as the η-mapping of the flow Φ of $\hat{S}(p,x_2)$.

The set $\mathcal{H}$ is represented in both the p-x_2 phase plane of $\hat{S}(p,x_2)$ and in the x_1-x_2 phase plane of $S(x_1,x_2)$ by the lines $x_2 = h \in \mathcal{H}$. The non-diffeomorphic nature of η manifests itself in the behavior of the trajectories $\Psi'(t)$ crossing the line $x_2 = h$.

Define the point set

$$Q \triangleq \left\{(x_1,x_2) \in \mathbb{R}^2 : x_1 = a_0 + \sum_{k=1}^{m} a_k\, T_k(x_2),\ x_2 \in \mathcal{H}\right\} \qquad (46$$

For each line $x_2 = h$, there is exactly one point $(x_1,x_2) \in Q$.

Lemma 4.

Let $\Psi'(t) = (x_1(t),\ x_2(t))$ be a trajectory of $S(x_1,x_2)$ so that $x_2(\tau) = h \in \mathcal{H}$, for some $\tau \in \mathbb{R}$. Then $\Psi'(\tau) \in Q$.

Proof. If $x_2(\tau) \in \mathcal{H}$, then $\sum_{k=1}^{m} b_k U_{k-1}(x_2(\tau)) = 0$ and the lemma follows from (41) and (42). ◻

Lemma 4 asserts that the function η maps the lines $x_2 = h$ in the p-x_2 phase plane into the corresponding point $(x_1,x_2) \in Q$ in the x_1-x_2

phase plane. Hence we call the lines $x_2 = h \in \mathcal{H}$ barrier lines and the points $(x_1,x_2) \in Q$ tunnel points. Any trajectory of $S(x_1,x_2)$ attempting to cross a barrier line must do so at a tunnel point.

Example 3.

Let the limit cycle of $S(x_1,x_2)$ have as its first component

$$x_1(t) = \cos t + 2 \sin t + \frac{1}{2} \sin 2t \tag{47}$$

Then (41) becomes

$$x_1 = x_2 + p(x_2+2) \tag{48}$$

In this example, $\mathcal{H} = \{-2\}$, and $Q = \{(-2,-2)\}$. The trajectories of $S(x_1,x_2)$ displayed on the graphics display terminal are shown in Figure 6a.

Example 4.

Let the limit cycle of $S(x_1,x_2)$ have as its first component

$$x_1(t) = 2 \cos t + \sin t + \sin 25 \tag{49}$$

Then (41) becomes

$$x_1 = 2x_2 + p(1+2x_2) \tag{50}$$

Here, $\mathcal{H} = \{-.5\}$, $Q = \{-1,-.5)\}$. The expression (49) of this example is the same as that of Example 1. The display illustrating trajectories of $S(x_1,x_2)$ is shown in Figure 6b.

Example 3 illustrates a set of trajectories passing once through a tunnel point, while Example 4 illustrates a set of trajectories passing infinitely many times through a tunnel point. The number of times a trajectory passes through a tunnel point depends upon its x_2-component of motion, and hence upon the x_2-component of motion of the trajectories of $\hat{S}(p,x_2)$. An examination of (11) implies;

1) for all $|x_2| > \sqrt{\frac{1+\sqrt{2}}{2}}$, we have $\dot{x}_2/x_2 < 0$, and barrier lines in this region will have trajectories tunneling through them exactly once (Example 3),

2) for all $|x_2| \leq 1$, all non-constant solutions tend towards the limit cycle as $t \to \infty$. Along the limit cycle the x_2-component of motion is $\cos \omega t$. Hence any barrier line in this region will have trajectories tunneling through them in both directions $\dot{x}_2/x_2 > 0$ and $\dot{x}_2/x_2 < 0$ an infinite number of times (Example 4),

3) for the remaining region $1 < |x_2| \leq \sqrt{\frac{1+\sqrt{2}}{2}}$, qualitative examination of the trajectories of $\hat{S}(p,x_2)$ (Figure 7a) yields the conclusion that all trajectories mimic the motion of the limit cycle and rotate in a clockwise manner. Thus any barrier line in this region may be traversed by trajectories obeying $\dot{x}_2/x_2 > 0$ and $\dot{x}_2/x_2 < 0$. However, since the limit cycle does not lie in this region, the phenomenon of repeated tunneling will occur only a finite number of times.

For a general illustration of the η-transformation of $\hat{S}(p,x_2)$ to $S(x_1,x_2)$, see Figure 7. Throughout the remainder of this section we relate the trajectories of $S(x_1,x_2)$ to the solutions of a differential equation.

Theorem 2.

Let $\mathcal{H}$ be empty. Then the real, second-order, autonomous differential equation

$$\dot{x}_1 = \omega\left\{\left[x_2 + p(1-p^2 - x_2^2)\right]\left[\sum_{k=1}^{m} b_k\, U_{k-1}(x_2)\right] + \left[-p + x_2(1-p^2-x_2^2)\right]\left[\sum_{k=1}^{m} a_k \frac{d\, T_k(x_2)}{d\, x_2} + p\, b_k \frac{d\, U_{k-1}(x_2)}{d\, x_2}\right]\right\} \qquad (51)$$

$$\dot{x}_2 = \omega\{-p + x_2\,(1-p^2-x_2^2)\} \qquad (52)$$

where p is defined in (44) has unique solutions which are members of $S(x_1,x_2)$. Furthermore, every trajectory of $S(x_1,x_2)$ is a solution of (51), (52) with initial condition $(p(0),x_2(0)) = \eta^{-1}(x_1(0),x_2(0))$.

Proof. The proof follows in the same manner as the proof of Theorem 1. ◻

If $\mathcal{H}$ is not empty, then p in (44) is not defined for all $x_2 = h \in \mathcal{H}$ because the denominator in (44) is zero. Consequently (51) and (52) are defined only for $x_2 \notin \mathcal{H}$. That is, (51) and (52) generate a vector field in the x_1-x_2 phase plane that is defined everywhere except at the barrier lines. We say that trajectory $\Psi(t)$, $\Psi\colon \mathbb{R} \to \mathbb{R}^2$, satisfies (51) and (52) if it is every where tangent to the vector field defined by (51) and (52).

Corollary 2.[3]

Let Ψ be a continuous trajectory in $\mathbb{R}^2$; $\Psi(t)$ is defined for $t \in [t_1,t_2]$. Let $x_2(t)$ be the second component of $\Psi(t)$ and $x_2(t) \notin \mathcal{H}$ for all $t \in [t_1,t_2]$. Then Ψ satisfies (51) and (52) if and only if $\Psi(t) = \eta(\Phi(t,(p(0),x_2(0)))$ for some initial condition $(p(0),x_2(0)) \in \mathbb{R}^2$.

Proof. Since Ψ never intersects a barrier line by hypothesis, (51) and (52) are well-defined for all $t \in [t_1,t_2]$ and hence the proof is the same as that of Theorem 1. ¤

Corollary 2 asserts that the vector field generated by (51) and (52) is the η-image of the vector field of $\hat{S}(p,x_2)$ for all $x_2 \notin \mathcal{H}$.

Lemma 5.

Let Ψ be a trajectory in $\mathbb{R}^2$ defined for $t \in [t_1,t_2]$ such that there exists exactly one time τ when the second component of Ψ satisfies $x_2(\tau) \in \mathcal{H}$, and $\tau \in (t_1,t_2)$. Then we have:

A. Ψ is continuous and satisfies (51) and (52) if and only if:

(i) $\Psi(t) = \eta(\Phi(t,(p(0),x_2(0)))$ (53)

for $t \in [t_1,\tau)$, for some $(p(0),x_2(0)) \in \mathbb{R}^2$

(ii) $\Psi(\tau) \in Q$ (54)

[3]This corollary, as well as Lemma 5 and Theorem 3 that follow are designed to relate the trajectories Ψ' of $S(x_1,x_2)$ to (51) and (52) under the assumption that $\mathcal{H}$ is not empty. However trajectory Ψ in Corollory 2 and Lemma 5 is not necessarily an element of $S(x_1,x_2)$.

and

(iii) $\Psi(t) = \eta(\Phi(t,(p'(0),x_2'(0)))$ (55)

for $t \in (\tau,t_2]$, for some $(p'(0),x_2'(0)) \in \mathbb{R}^2$

B. If the elements of $\mathcal{H}$ are simple zeroes of $\sum_{k=1}^{m} b_k U_{k-1}(x_2)$, then Ψ is a C^1 trajectory if and only if $(p(0),x_2(0)) = (p'(0),x_2'(0))$.

Proof. A. Equations (51) and (52) are not defined at $t = \tau$. But for any $\varepsilon > 0$, Corollary 2 may be applied for $t \in [t_1,\tau - \varepsilon]$. Letting $\varepsilon \to 0$ demonstrates (53), and a similar argument demonstrates (55). Lemma 4, (53) and (55) imply (54).

B. It is only necessary to examine the C^1 continuity at $t = \tau$. Let $x_1(t)$, $x_2(t)$ be the first and second components of $\Psi(t)$ respectively. Requiring Ψ to be C^1 continuous at $t = \tau$ is equivalent to requiring[4]

$$\lim_{\varepsilon \to 0} \left(\frac{\dot{x}_1(\tau - \varepsilon)}{\dot{x}_2(\tau - \varepsilon)} \right) = \lim_{\varepsilon \to 0} \left(\frac{\dot{x}_1(\tau + \varepsilon)}{\dot{x}_2(\tau + \varepsilon)} \right) \tag{56}$$

Let (p,x_2) and (p',x_2') be the components of $\Phi(t,(p(0),x_2(0)))$ and $\Phi(t,(p'(0),x_2'(0)))$ respectively. Part A of this Lemma asserts $x_2(\tau) = x_2'(\tau) = h \in \mathcal{H}$. Using (51) and (52), equation (56) becomes

[4]Observe that (56) is well defined even if $\dot{x}_2(\tau) = 0$ because the continuity of Ψ and equation (51) imply $\dot{x}_1(\tau) = 0$. Hence L'Hospital's rule may be used.

$$\sum_{k=1}^{m} \left[a_k d \frac{T_k(x_2(\tau))}{dx_2} + p(\tau) b_k d \frac{U_{k-1}(x_2(\tau))}{dx_2} \right] =$$

$$\sum_{k=1}^{m} \left[a_k d \frac{T_k(x_2'(\tau))}{dx_2'} + p'(\tau) b_k d \frac{U_{k-1}(x_2(\tau))}{dx_2'} \right] \qquad (57)$$

Since $\sum_{k=1}^{m} b_k U_{k-1}(x_2)$ has only simple zeroes, (57) is valid if and only if $p'(\tau) = p(\tau)$. Thus $(p(\tau), x_2(\tau)) = (p'(\tau), x_2'(\tau))$ and hence $(p(0), x_2(0)) = (p'(0), x_2'(0))$ by the uniqueness of solutions of $\hat{S}(p, x_2)$. ¤

Part A of Lemma 5 demonstrates the tunneling effect--all continuous Ψ satisfying (51) and (52) intersect barrier lines at the tunnel points. Part B of Lemma 5 implies

Theorem 3.

Let the elements of $\mathcal{H}$ be simple zeroes of the polynomial $\sum_{k=1}^{m} b_k U_{k-1}(x_2)$. Let $(x_1(0), x_2(0)) \in \mathbb{R}^2$, $x_2(0) \notin \mathcal{H}$. Then there exists a unique C^1 function Ψ satisfying (51) and (52) and satisfying $\Psi(0) = (x_1(0), x_2(0))$. This function Ψ is a member of $S(x_1, x_2)$ where $(p(0), x_2(0))$ in (45) is given by

$$(p(0), x_2(0)) = \eta^{-1}(x_1(0), x_2(0)). \qquad (58)$$

Proof. Equation (58) is well-defined since $x_2(0) \notin \mathcal{H}$. Since Ψ is continuous and $\mathcal{H}$ has a finite number of elements, along any time interval $[0,t]$ either Ψ obeys Corollary 2 or else the interval $[0,t]$ may be broken into a finite sequence of sub-intervals $\{[t_j, t_{j+1}]\}_{j=1}^{n}$ such that Lemma 5 may be applied to each sub-interval. In any sub-interval, $\Psi \in C^1$ if and only if part B of Lemma 5 is satisfied. Thus in every interval, $(p(0), x_2(0)) = (p'(0), x_2'(0)) = \eta^{-1}(x_1(0), x_2(0))$. ¤

The requirement that $\mathcal{H}$ contains only simple zeroes of $\sum_{k=1}^{m} b_k U_{k-1}(x_2)$ is of no practical importance because (2) is only an approximation of (1) and can be modified. Thus Theorem 3 answers the question posed in the Introduction concerning the minimum number of state variables required to generate (2); the trajectories of $S(x_1, x_2)$ are the unique C^1 solutions of (51), (52). This conclusion has more than theoretical importance. Most integration algorithms in digital computers assume a C^1 solution. The waveforms in Figure 6 illustrating Example 3 and Example 4 were generated by (51) and (52). Similarly, the Pukinje fiber cell waveform of Example 2 was successfully reproduced by (51) and (52) on a digital computer and in this case the set $\mathcal{H}$ contained many elements.

VI. CONCLUDING REMARKS

We have shown that $S(x_1,x_2,x_3)$ has (2) as its limiting solution, and that (51) and (52) have (2) as the unique C^1 limiting solution. However it is our opinion that the best method to generate (2) is that illustrated in Figure 1b--generating sin ωt and cos ωt by $\hat{S}(p,x_2)$ and using (7) to produce (2). This method is simple and has the distinct advantage of separating the limit-cycle qualities of $\hat{S}(p,x_2)$ in Block 1' from the polynomial generator Block 2. It is possible to alter the constants a_k and b_k of (2) by adjusting the variable resistances shown in Figure 3. This flexibility is not found with the other methods because the polynomial (7) is intertwined with the differential equations.

At the present time we are studying differential equations similar to (51) and (52) which 1) extract both sub-harmonics and harmonics of a given periodic function, and 2) reproduce a given limit cycle in $\mathbb{R}^2$.

Lastly, there has been no comment concerning the types of transient phenomena of the trajectories of $S(x_1,x_2)$ or $S(x_1,x_2,x_3)$. Here we note two aspects concerning transient responses; these systems have two or three different sets of initial conditions all of which prescribe the transient phenonema. Secondly, there are an infinite number of different types of systems $\hat{S}(p,x_2)$ all having the same limit cycle solution. For instance we could replace the term $(1-p^2-x_2^2)$ by $(1-p^2-x_2^2)^{2n+1}$ for any $n \geq 1$, thus changing the rate of decay of the transient solution without affecting the steady-state.

ACKNOWLEDGEMENT

We thank Mr. Raymond Lee for his help in implementing a digital analysis of the Purkinje fiber cell example.

REFERENCES

[1] P. Hartman, Ordinary Differential Equations, New York: John Wiley, 1964.

[2] N. Minorsky, Nonlinear Oscillation. New York: D. Van Nostrand, 1962.

[3] V. V. Nemytskii and V. V. Stepanov, Qualitative Theory of Differential Equations, N. J.: Princeton University Press, 1960.

[4] G. Sansone and R. Conti, Nonlinear Differential Equations. New York: Pergamon Press, 1964.

[5] A. A. Andronov, A. A. Vitt, and S. E. Khaikin, Theory of Oscillators. Reading, Mass.: Addison-Wesley, 1966.

[6] L. M. Vallese, "On the synthesis of nonlinear systems," in Proc. Symp. Nonlinear Circuit Analysis. New York: Polytechnic Institute of Brooklyn Press, 1953, pp. 201-214.

[7] C. A. Desoer and B. Peikari, "Design of linear time-varying and nonlinear time-invariant networks," IEEE Trans. Circuit Theory, vol. CT-17, pp. 232-240, May 1970.

[8] L. O. Chua, "Synthesis of nonlinear systems with prescribed singularities," IEEE Trans. Circuit Theory, vol. CT-18, pp. 375-382, May 1971.

[9] B. Peikari, "Design of nonlinear networks with a prescribed small-signal behavior," IEEE Trans. Circuit Theory, vol. CT-19, pp. 389-391.

[10]. S. C. Bass, "Transient waveform generation with lumped, nonlinear, dynamic networks," IEEE Trans. Circuit Theory, vol. CT-19, pp. 544-554, November 1972.

[11] L. O. Chua, Introduction to Nonlinear Network Theory. New York: McGraw-Hill, 1969.

[12] D. Noble, "A modification of the Hodgkin-Huxley equations applicable to Purkinje fiber action and pacemaker potentials," J. Physiol., vol. 160, pp. 317-352, 1962.

[13] Y. Omura, "The relationship between the transmembrane action potential and the voltage-time-dependent, negative resistance characteristics of the voltage-current curves of excitable pacemaker and non-pacemaker cell membranes," The New York Academy of Sciences, Series II, vol. 33, no. 5, pp. 467-504, May 1971.

[14] R. FitzHugh, "Mathematical models of excitation and propagation in nerve," in Biological Engineering, edited by H. P. Schwan, New York: McGraw-Hill, pp. 1-85.

[15] T. Pavlidis, "Studies of biological clocks: a model for the circadian rhythms of nocturnal organisms," in Some Mathematical Problems in Biology, Providence, Rhode Island, The American Mathematical Society, pp. 88-112, 1966.

[16] A. B. Grebene, "Monolithic waveform generation," IEEE Spectrum, pp. 34-40, April 1972.

[17] J. Eimbinder, Application Considerations for Linear Integrated Circuits, New York: John Wiley, 1970.

[18] L. Fox and I. B. Parker, Chebyshev Polynomials in Numerical Analysis. London: Oxford University Press, 1968.

[19] Continuous Systems Modeling Program (CSMP): A digitally simulated analog computer or a DSC META-IV 16K computer with IBM 2250 Interactive Graphics package.

FIGURE CAPTIONS

Fig. 1. (a) Block diagram of the system transforming the output of the function generator to the desired waveform. (b) Block diagram illustrating the autonomous generation of the desired waveform.

Fig. 2. Detailed diagram illustrating Block 1.

Fig. 3. Detailed diagram illustrating Block 2.

Fig. 4. (a) Photograph of analog diagram on the CSMP used to simulate $S(x_1,x_2,x_3)$ of Example 1. (b) Periodic waveform $x_1(t)$ of Example 1.

Fig. 5. Transmembrane action potential of the Cardiac Purkinje Fiber.

Fig. 6. Trajectories of $S(x_1,x_2)$ (a) Example 3 and (b) Example 4.

Fig. 7. Illustration of the η-mapping of the trajectories of $\hat{S}(p,x_2)$ to the trajectories of $S(x_1,x_2)$.

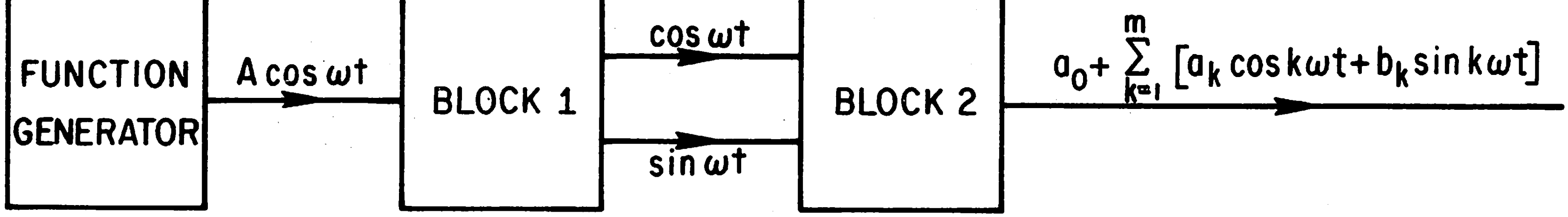
FUNCTION GENERATOR
A cos ωt
BLOCK 1
cos ωt
sin ωt
BLOCK 2
$a_0+\sum_{k=1}^{m}[a_k\cos k\omega t+b_k\sin k\omega t]$

(a)

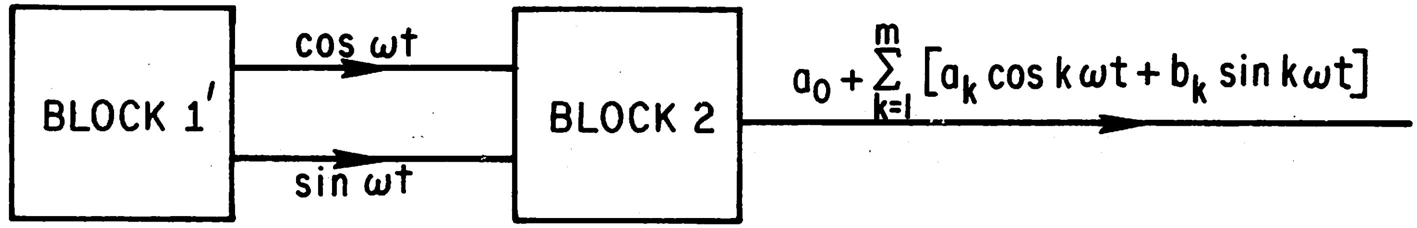
BLOCK 1′
cos ωt
sin ωt
BLOCK 2
$a_0+\sum_{k=1}^{m}[a_k\cos k\omega t+b_k\sin k\omega t]$

(b)

Fig. 1

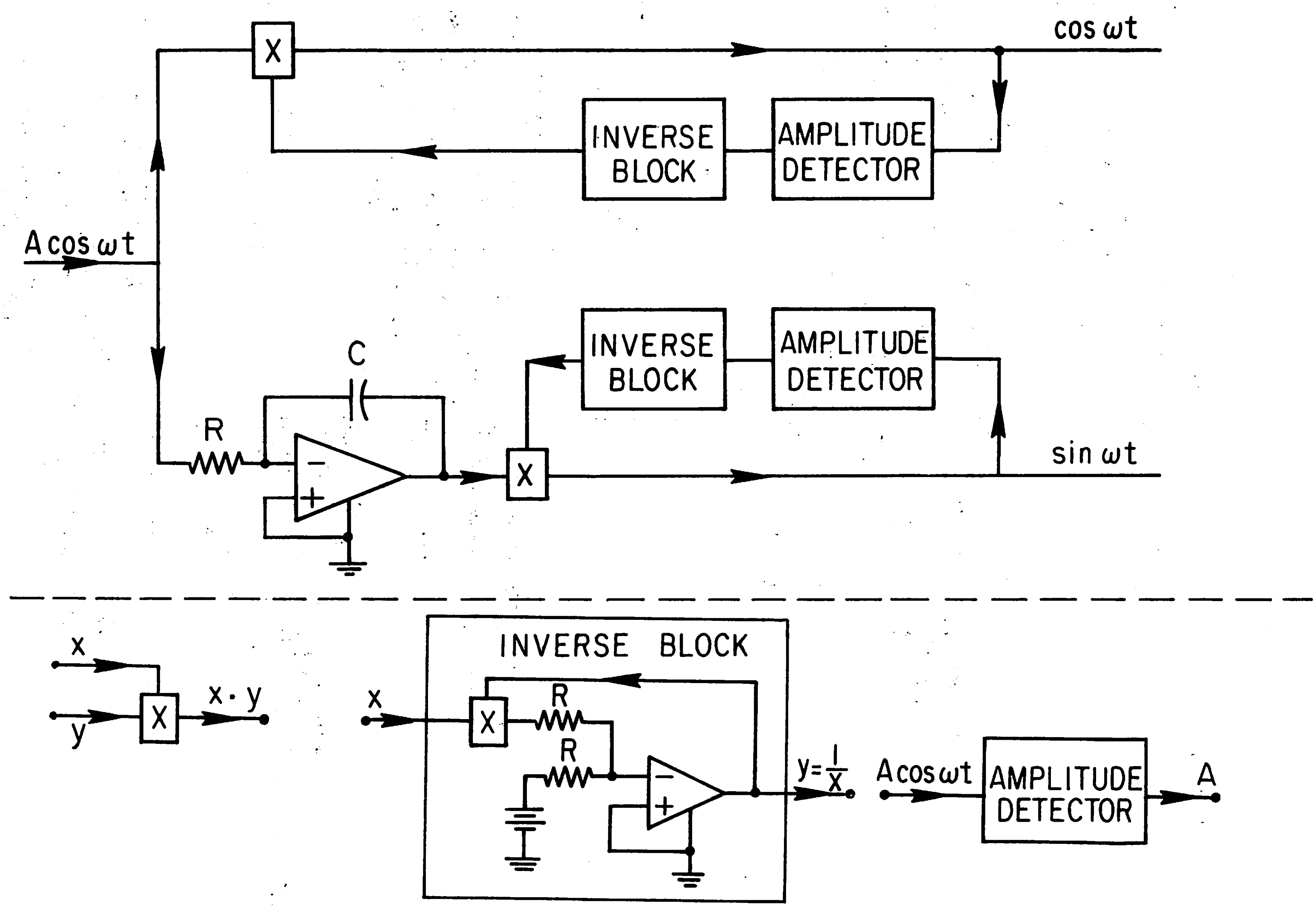

cos ωt
INVERSE BLOCK
AMPLITUDE DETECTOR
A cos ωt
C
R
INVERSE BLOCK
AMPLITUDE DETECTOR
sin ωt
x
y
x · y
X
INVERSE BLOCK
x
R
R
y = 1/x
A cos ωt
AMPLITUDE DETECTOR
A

Fig. 2

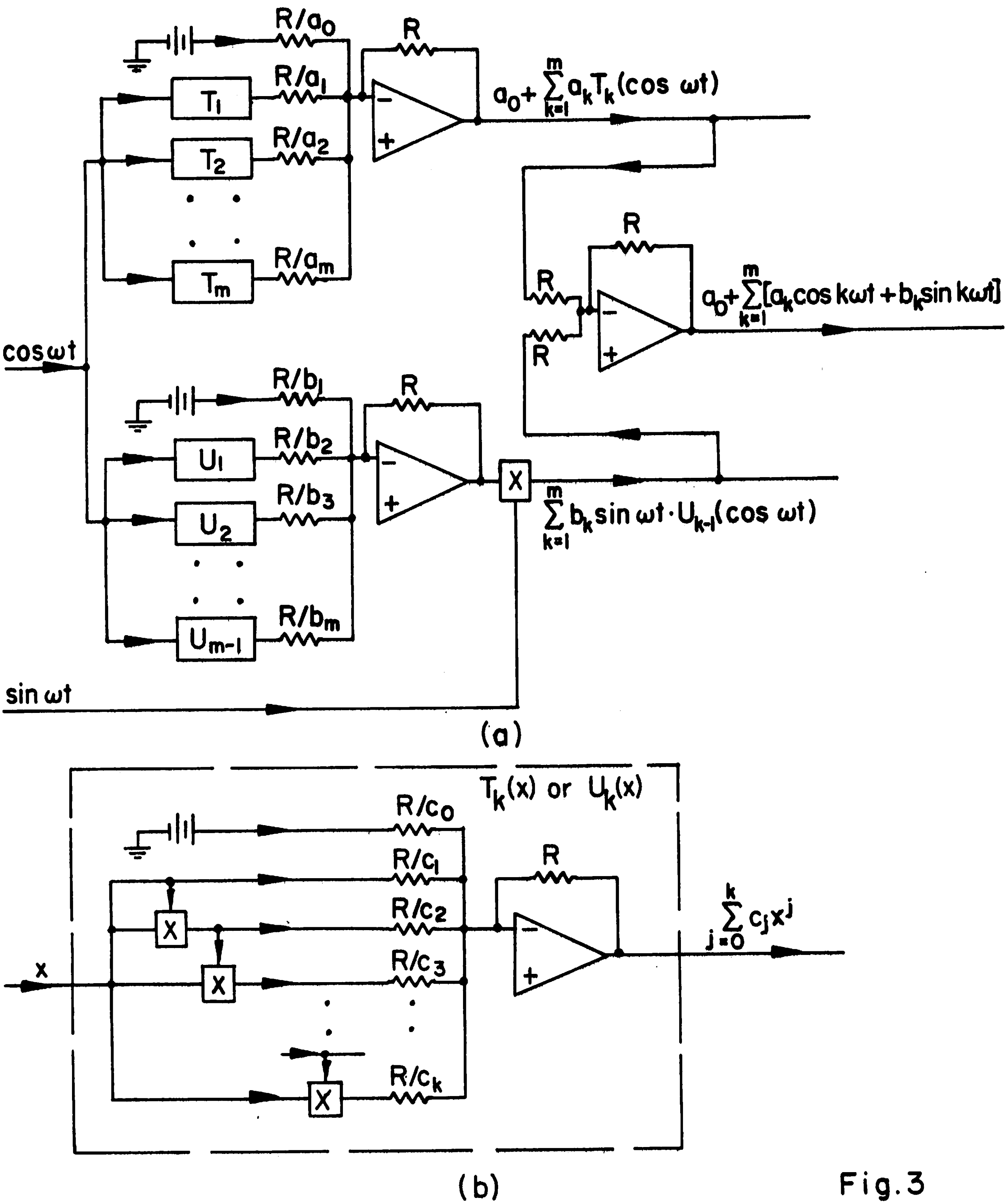
R/a0
R
T1
R/a1
a0+ Σ_{k=1}^{m} a_k T_k (cos ωt)
T2
R/a2
Tm
R/am
R
R
R
a0+ Σ_{k=1}^{m} [a_k cos kωt + b_k sin kωt]
cos ωt
R/b1
R
U1
R/b2
U2
R/b3
X
Σ_{k=1}^{m} b_k sin ωt · U_{k-1}(cos ωt)
Um-1
R/bm
sin ωt
(a)
Tk(x) or Uk(x)
R/c0
R/c1
R
R/c2
X
Σ_{j=0}^{k} c_j x^j
x
X
R/c3
X
R/ck
(b)

Fig.3

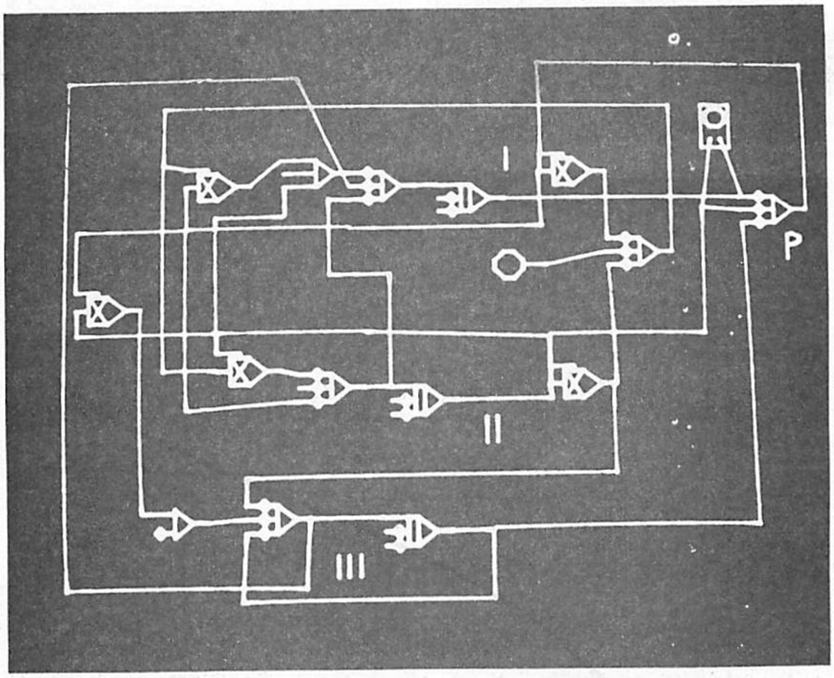

(a)

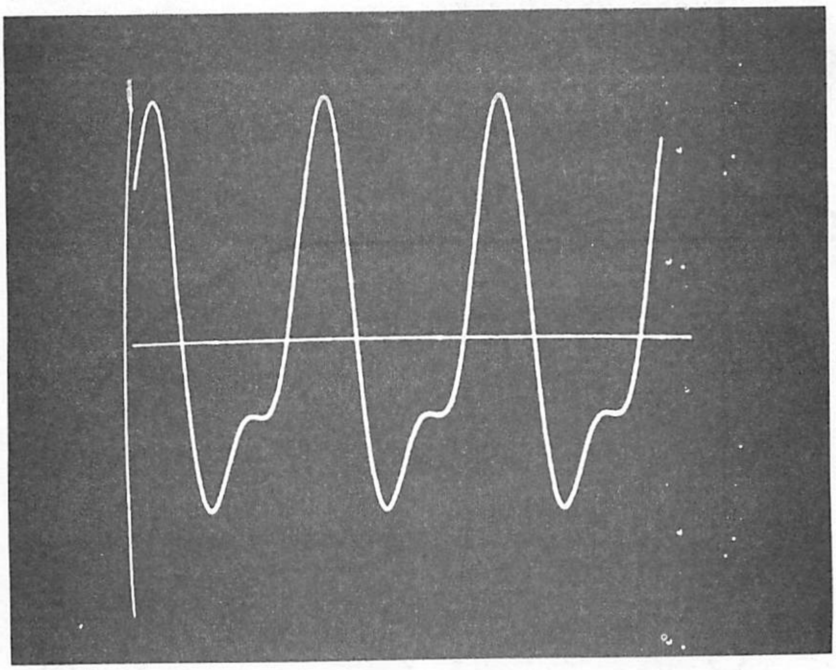

(b)

Fig. 4

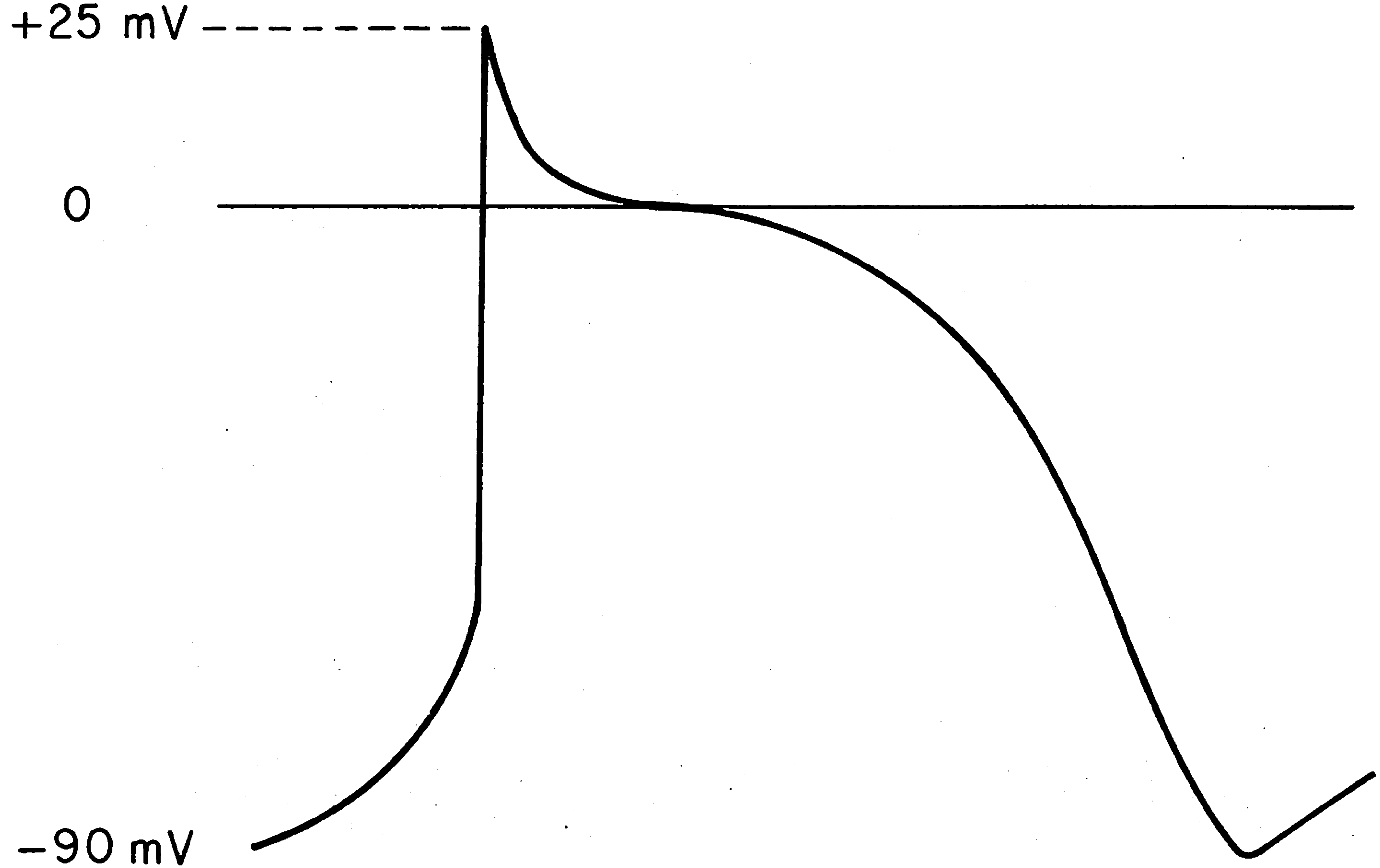

Fig. 5

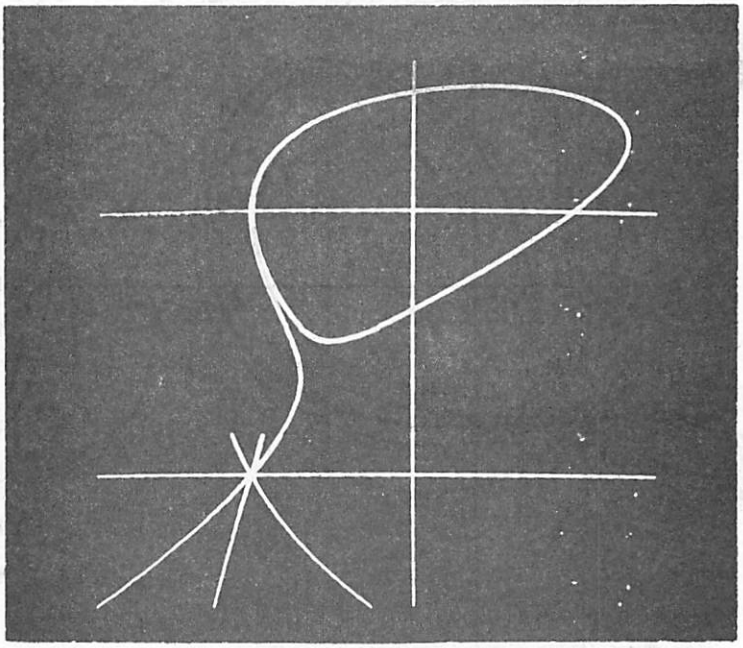

(a)

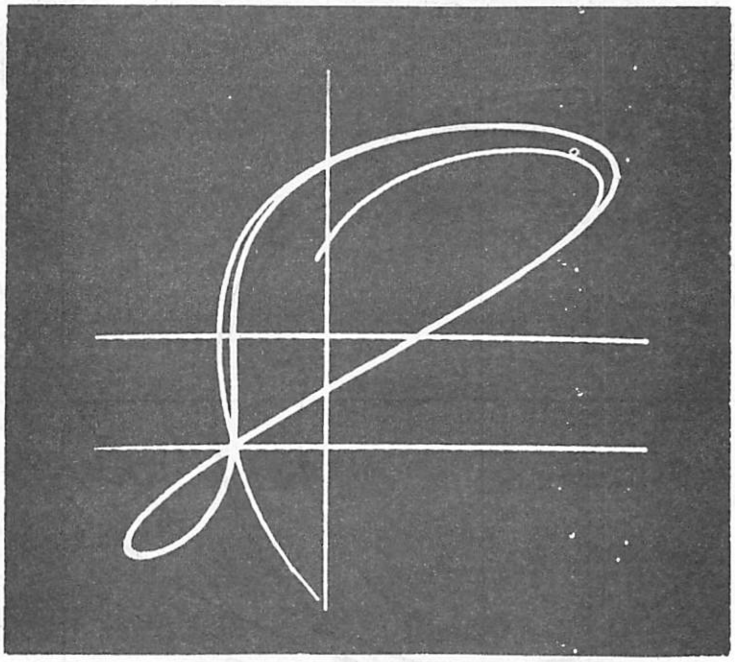

(b)

Fig. 6

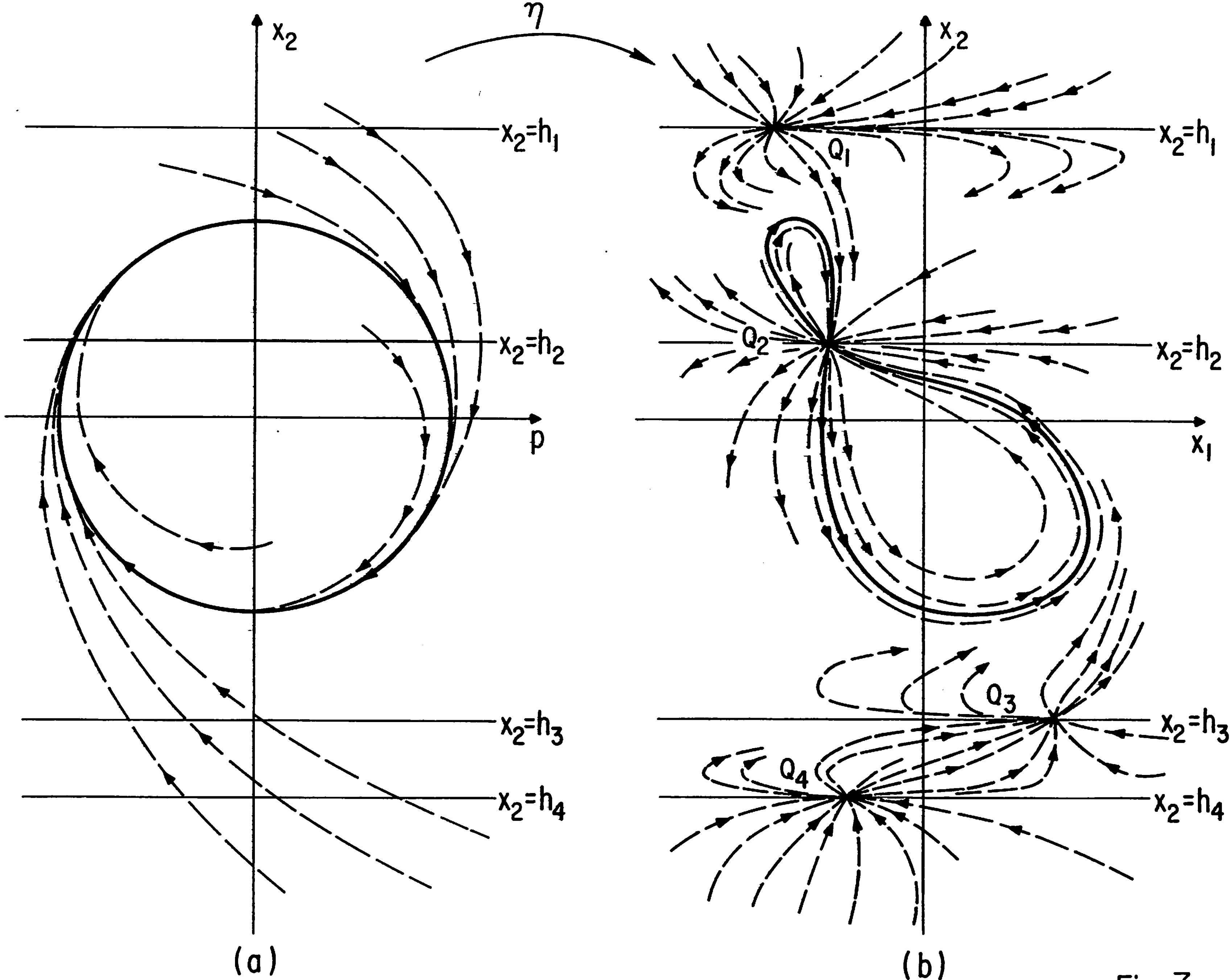
x2
x2=h1
x2=h2
p
x2=h3
x2=h4
(a)
η
x2
Q1
x2=h1
Q2
x2=h2
x1
Q3
x2=h3
Q4
x2=h4
(b)

Fig. 7